

## Supporting Information

### Metal-organic framework derived carbon supported Cu-In bimetallic nanoparticles for highly selective CO<sub>2</sub> electroreduction to CO

Xia Ma<sup>a,b</sup>, Jianjian Tian<sup>a,b</sup>, Min Wang<sup>a,b</sup>, Xixiong Jin<sup>a,b</sup>, Meng Shen<sup>a,b</sup>, Lingxia Zhang<sup>\*a,b,c</sup>

<sup>a</sup> State Key Laboratory of High Performance Ceramics and Superfine Microstructure, Shanghai Institute of Ceramics, Chinese Academy of Sciences, 1295 Ding-xi Road, Shanghai, 200050, P. R. China

<sup>b</sup> Center of Materials Science and Optoelectronics Engineering, University of Chinese Academy of Sciences, No. 19A Yuquan Road, Beijing 100049, P. R. China

<sup>c</sup> School of Chemistry and Materials Science, Hangzhou Institute for Advanced Study, University of Chinese Academy of Sciences, 1 Sub-lane Xiangshan, Hangzhou 310024, P. R. China

\*Corresponding author. E-mail: zhlingxia@mail.sic.ac.cn

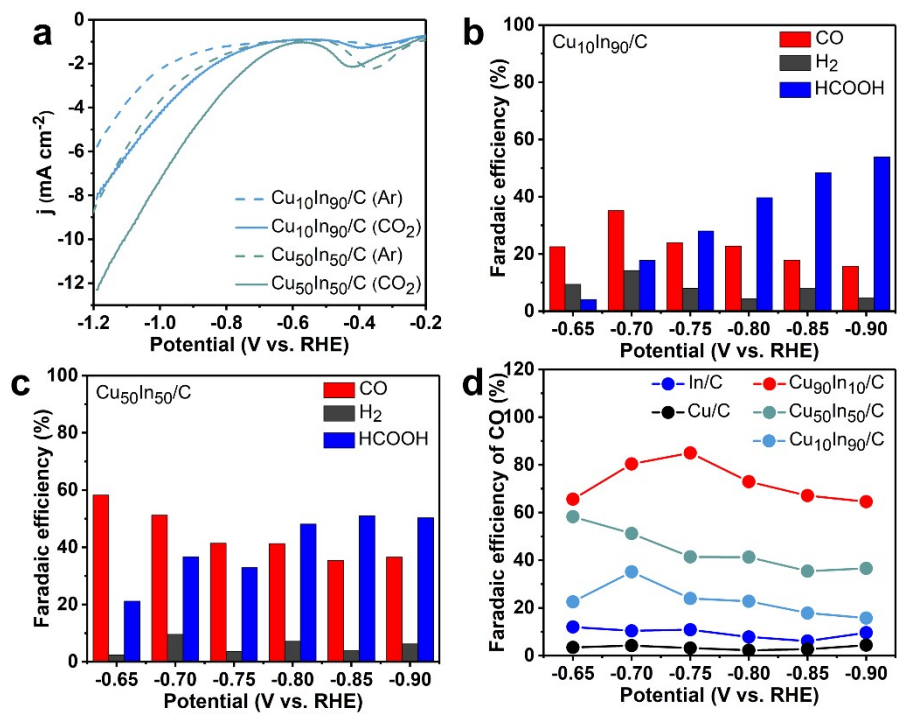


**Fig. S1** LSV curves (a) and products selectivity on  $\text{Cu}_{10}\text{In}_{90}/\text{C}$  (b) and  $\text{Cu}_{50}\text{In}_{50}/\text{C}$  (c).

Faradaic efficiency of CO on  $\text{Cu}_x\text{In}_{100-x}/\text{C}$  (d).

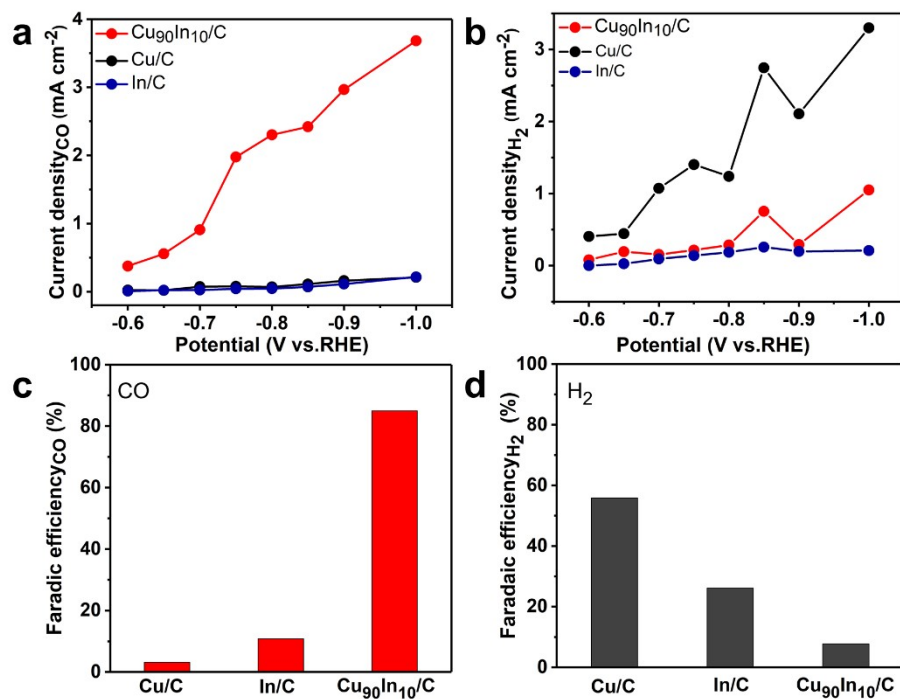


**Fig. S2** Current density of CO (a) and H<sub>2</sub> (b) at -0.6 V ~ -1.0 V, and Faradaic efficiency of CO (c) and H<sub>2</sub> (d) at the potential of -0.75 V on Cu/C, In/C and Cu<sub>90</sub>In<sub>10</sub>/C catalysts.

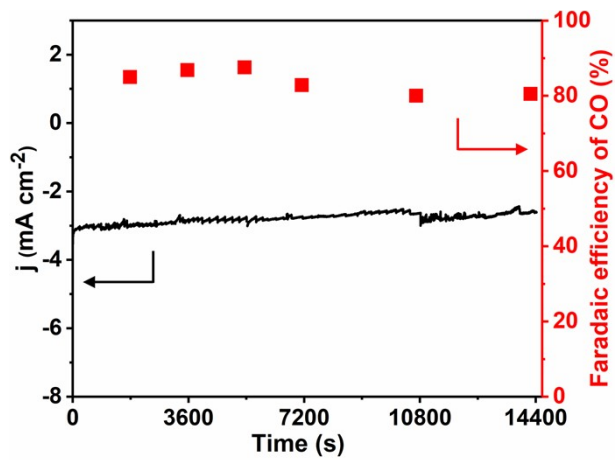


**Fig. S3** The stability of  $\text{Cu}_{90}\text{In}_{10}/\text{C}$  at -0.75 V.

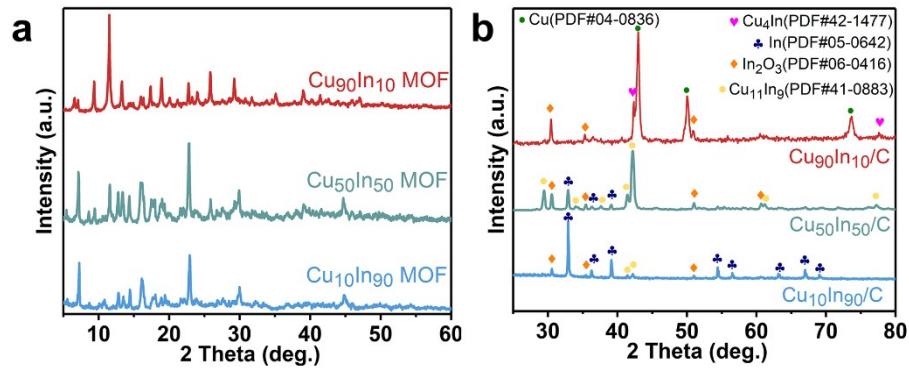


**Fig. S4** XRD patterns of  $\text{Cu}_x\text{In}_{100-x}$  MOFs (a) and  $\text{Cu}_x\text{In}_{100-x}/\text{C}$  (b).

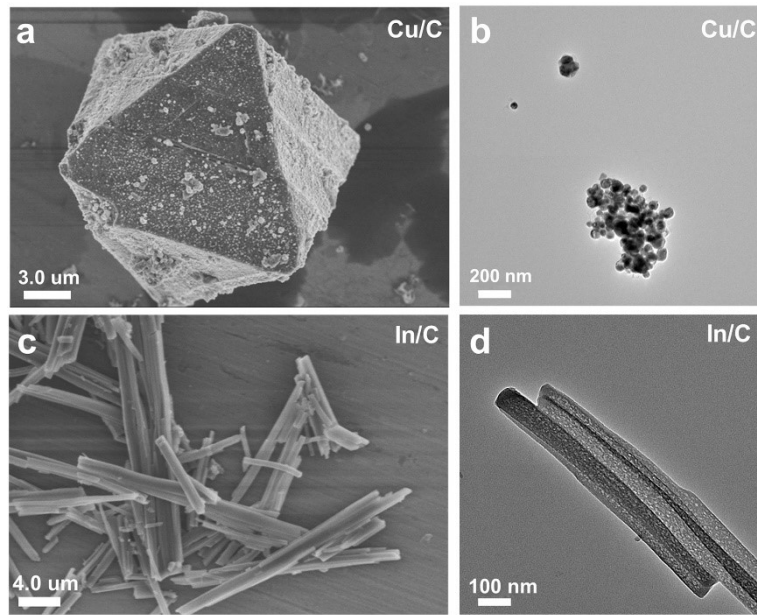


**Fig. S5** SEM and TEM images of Cu/C (a, b) and In/C (c, d).

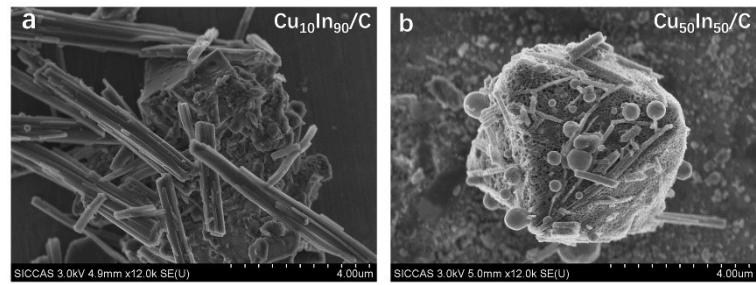


**Fig. S6** SEM images of Cu<sub>10</sub>In<sub>90</sub>/C (a) and Cu<sub>50</sub>In<sub>50</sub>/C (b).

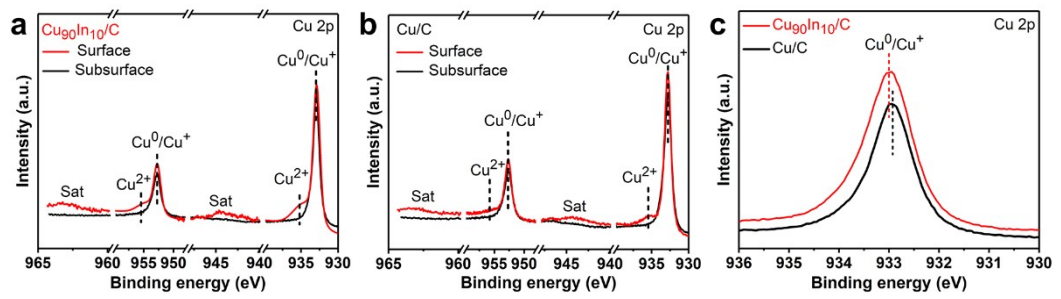


**Fig. S7** The Cu 2p XPS spectra on the surface and subsurface of  $\text{Cu}_{90}\text{In}_{10}/\text{C}$  (a) and  $\text{Cu}/\text{C}$  (b), the comparison of  $\text{Cu} 2p_{3/2}$  peaks of  $\text{Cu}_{90}\text{In}_{10}/\text{C}$  and  $\text{Cu}/\text{C}$ .

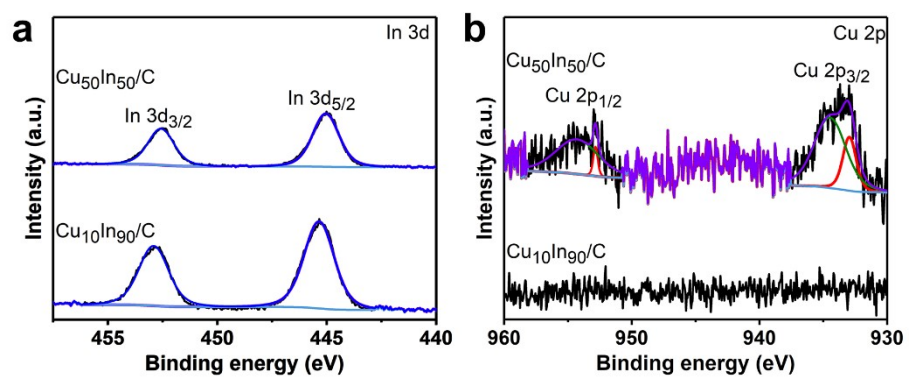


**Fig. S8** In 3d (a) and Cu 2p (b) XPS spectra of Cu<sub>10</sub>In<sub>90</sub>/C and Cu<sub>50</sub>In<sub>50</sub>/C.

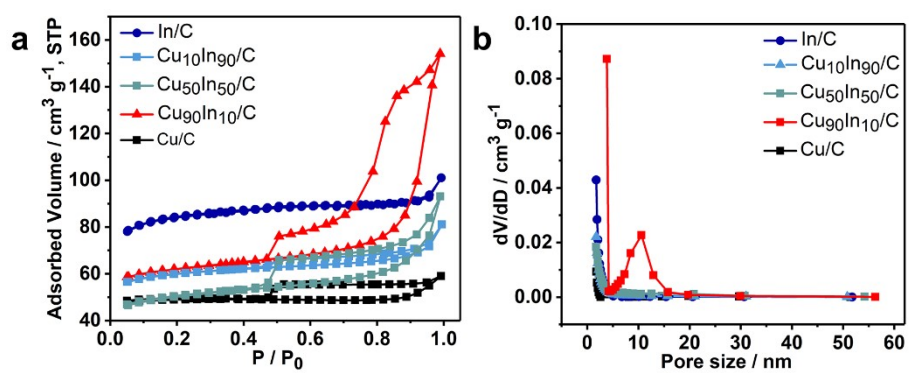


**Fig. S9**  $\text{N}_2$  adsorption isotherms (a) and pore size distributions (b) of  $\text{Cu}_x\text{In}_{100-x}/\text{C}$ .

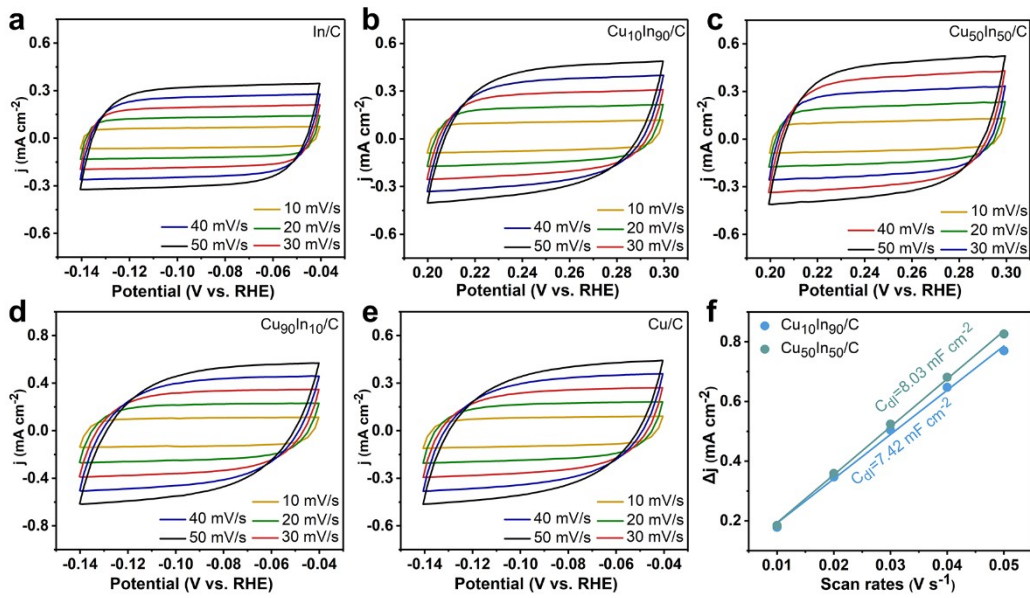


**Fig. S10** CV curves of  $\text{Cu}_x\text{In}_{100-x}/\text{C}$  obtained at various scan rates (a-e), charging current density differences plotted against scan rates of  $\text{Cu}_{10}\text{In}_{90}/\text{C}$  and  $\text{Cu}_{50}\text{In}_{50}/\text{C}$  (f).

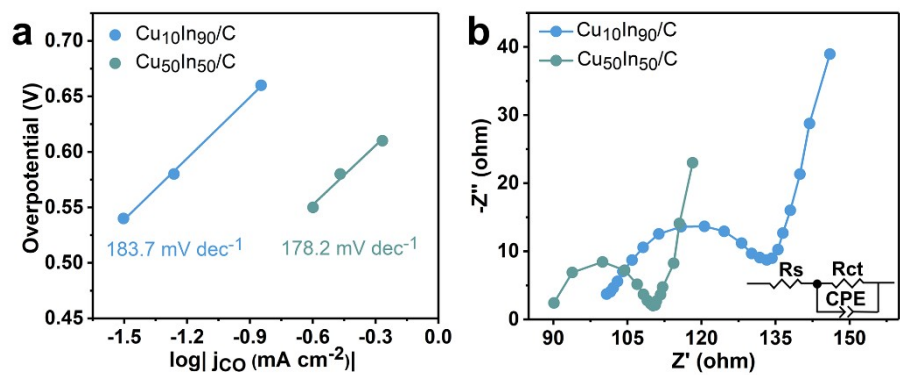


**Fig. S11** Tafel plots for CO (a), and Nyquist plots (b) of  $\text{Cu}_{10}\text{In}_{90}/\text{C}$  and  $\text{Cu}_{50}\text{In}_{50}/\text{C}$ .

**Table S1.** The atom ratio of Cu<sub>90</sub>In<sub>10</sub>/C measured by ICP-OES.

Elements	At (%)
Cu	1.03
In	0.093
<b>Cu/In</b>	<b>11.07</b>

**Table S2.** Comparison of FE<sub>CO</sub> on Cu<sub>90</sub>In<sub>10</sub>/C with other reported Cu-based MOFs catalysts.

Catalyst	Electrolyte	Maximum FE <sub>CO</sub> (%)	Potential (V vs. RHE)/ J (mA cm <sup>-2</sup> )
Cu <sub>90</sub> In <sub>10</sub> /C (this work)	0.1 M KHCO <sub>3</sub>	95	-0.75/-2.3
C-Cu(OH) <sub>2</sub> @ZIF-8-10%-1000 <sup>1</sup>	0.5 M KHCO <sub>3</sub>	90	-0.5/~ -5
CoPc-Cu-O <sup>2</sup>	0.1 M KHCO <sub>3</sub>	85	-0.74/-13.2
Cu-NC400 <sup>3</sup>	0.1 M KHCO <sub>3</sub>	~ 23	-0.7/~ -2
Cu-MOF-74 derived Cu NPs <sup>4</sup>	0.1 M KHCO <sub>3</sub>	~ 5	-1.1/~ -3
Fe <sub>0.07</sub> Cu-N-C <sub>800</sub> <sup>5</sup>	--	47.8	-1.2 (V vs. Ag/AgCl) /~ -18
Cu-N-C <sub>1100</sub> <sup>6</sup>	0.1 M KHCO <sub>3</sub>	40.8	-0.6/~ -0.4
Cu <sub>2</sub> O@Cu-MOF <sup>7</sup>	0.1 M KHCO <sub>3</sub>	23.1	-0.91/~ -2.5
MOFs-driven Cu/Cu <sub>2</sub> O <sup>8</sup>	0.5 M KHCO <sub>3</sub>	43.8	-0.76/~ -22.5
Cu-N-C <sup>9</sup>	0.5 M KHCO <sub>3</sub>	~ 23	-0.55/~ -2
MOFs-derived Cu <sub>x</sub> O/C <sup>10</sup>	0.1 M KHCO <sub>3</sub>	~ 22.2	-0.78/--

## References

1. X. Chen, L. Ma, W. Su, L. Ding, H. Zhu and H. Yang, *Electrochim. Acta*, 2020, **331**, 135273.
2. Z. Meng, J. Luo, W. Li and K. A. Mirica, *J. Am. Chem. Soc.*, 2020, **142**, 21656-21669.
3. Y. Cheng, X. Chu, M. Ling, N. Li, K. Wu, F. Wu, H. Li, G. Yuan and X. Wei, *Catal. Sci. Technol.*, 2019, **9**, 5668-5675.
4. M. K. Kim, H. J. Kim, H. Lim, Y. Kwon and H. M. Jeong, *Electrochim. Acta*, 2019, **306**, 28-34.
5. S. Cao, H. Chen, M. Liu, B. Feng, B. Dong, Q. Zheng, W. Liu and Y. Teng, *J. CO<sub>2</sub> Util.*, 2021, **44**, 101418.
6. S. Cao, H. Chen, B. Dong, Q. Zheng, Y. Ding, M. Liu, S. Qian, Y. Teng, Z. Li and W. Liu, *J. Energy Chem.*, 2021, **54**, 555-563.
7. X. Tan, C. Yu, C. Zhao, H. Huang, X. Yao, X. Han, W. Guo, S. Cui, H. Huang and J. Qiu, *ACS Appl. Mater. Interfaces*, 2019, **11**, 9904-9910.
8. J. Liu, L. Peng, Y. Zhou, L. Lv, J. Fu, J. Lin, D. Guay and J. L. Qiao, *ACS Sustain. Chem. Eng.*, 2019, **7**, 15739-15746.
9. L. Jiao, W. J. Yang, G. Wan, R. Zhang, X. S. Zheng, H. Zhou, S. H. Yu and H. L. Jiang, *Angew. Chem., Int. Ed.*, 2020, **59**, 20589-20595.
10. K. Yao, Y. Xia, J. Li, N. Wang, J. Han, C. Gao, M. Han, G. Shen, Y. Liu, A. Seifitokaldani, X. Sun and H. Liang, *J. Mater. Chem. A*, 2020, **8**, 11117-11123.